THE JOURNAL OF PHYSICAL CHEMISTRY Letters

Letter

Cite This: J. Phys. Chem. Lett. 2019, 10, 7863−7869

pubs.acs.org/JPCL

Few-Layer PbI_2 Nanoparticle: A 2D Semiconductor with Lateral Quantum Confinement

Jinqiu Liu,[†] Yan Sun,[‡] Yong Zhou,[†] Chunfeng Zhang,[†] Xiaoyong Wang,*[,†] Lin Wang,*[,‡] and Min Xiao*[,†,§]

[†]National Laboratory of Solid State Microstructures, School of Physics, and Collaborative Innovation Center of Advanced Microstructures, Nanjing University, Nanjing 210093, China

[‡]Key Laboratory of Flexible Electronics, Institute of Advanced Materials, and Jiangsu National Synergetic Innovation Center for Advanced Materials, Nanjing Tech University, Nanjing 211816, China

[§]Department of Physics, University of Arkansas, Fayetteville, Arkansas 72701, United States

ABSTRACT: Inspired by the superior optoelectronic performances of various 2D semiconductors, their new compositions and structures are being actively pursued in order to foster novel fundamental physics and device applications. As a layered semiconductor with a direct bandgap, few-layer PbI_2 should have drawn much research attention due to their capability of emitting photons at short wavelengths of the visible spectrum. Here we chemically synthesize few-layer PbI_2 flakes and nanoparticles, which demonstrate unique exciton properties that have rare counterparts in other 2D semiconductors. For three layers and more, the single PbI_2 flakes can be utilized to show how the bandgap energy of a 2D semiconductor evolves with the changing layer thickness. The single PbI_2 nanoparticles are associated with an ultranarrow photoluminescence line width of ∼1 meV, thus reflecting the influence of lateral quantum confinement on the energy-level structures of a 2D semiconductor. The above findings mark the emergence of a potent 2D platform that is more than complementary to well-studied transition-metal dichalcogenide monolayers.

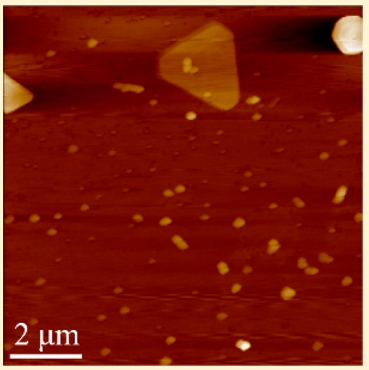

Owing to the ability to reduce material thickness down to the atomic scale, great research efforts have been devoted to various 2D materials with dramatically distinct optoelectronic properties from their bulk counterparts.[1,2] In the limit of monolayer thickness, graphene behaves like a semimetal with a negligible energy bandgap,[3] while hexagonal boron nitride exists to another extreme as an insulator useful for the encapsulation of functional nanodevices.[4] Meanwhile, atomically thin transition-metal dichalcogenides (TMDCs), which can be described by a general formula of MX_2, with M being a transition metal and X a chalcogen, work excellently as 2D semiconductors with optical emission spanning the visible to near-IR spectral range.[5,6] Aiming at ultimate applications in nanophotonics and optoelectronics, a rich spectrum of exciton physics has been discovered in monolayer TMDCs,[7−10] and pursuits of alternative compositions and structures are still being carried on after the appearances of black phosphorus,[11] perovskite nanosheets,[12] and other elemental 2D semiconductors.[13,14]

As a layered semiconductor with a direct bandgap,[15,16] the bulk form of lead iodide (PbI_2) is now being mainly used for the detection of nuclear radiation[17] and visible photons,[18,19] as well as for the synthesis of lead iodide perovskites in highly efficient solar cell devices.[20] For monolayer PbI_2, an indirect bandgap has been theoretically predicted[21−24] that is in great contrast to the direct one possessed by monolayer TMDCs. For three monolayers and more, a direct bandgap would be formed in few-layer PbI_2, with the optical emission reaching a much shorter wavelength range of the visible spectrum.[22−25] However, further explorations on the structural control and optical physics of few-layer PbI_2 materials are still needed, so that they can serve as a potent addition to the family of 2D semiconductors for the revelation of novel fundamental physics and practical applications.

In this Letter, we chemically synthesize and optically characterize 2D few-layer PbI_2 flakes at both room and cryogenic temperatures. At room temperature, the photoluminescence (PL) peak of PbI_2 flakes is shifted to the blue side with decreasing layer thickness, while the PL intensity is continuously decreased to reflect the transition from direct to indirect bandgaps. At the cryogenic temperature of 4 K, the trap-related emission becomes dominant in these PbI_2 flakes and gets saturated at high-power laser excitation. In addition to the above microsized flakes, we have also synthesized few-layer PbI_2 nanoparticles with a lateral dimension of ∼10 nm, which possess an ultranarrow PL line width of ∼1 meV at the cryogenic temperature. At high-power laser excitation, the optical signatures of both charged single excitons and neutral biexcitons can be observed from a single PbI_2 nanoparticle,

Received: October 14, 2019
Accepted: December 3, 2019
Published: December 3, 2019

DOI: 10.1021/acs.jpclett.9b03009
J. Phys. Chem. Lett. 2019, 10, 7863−7869

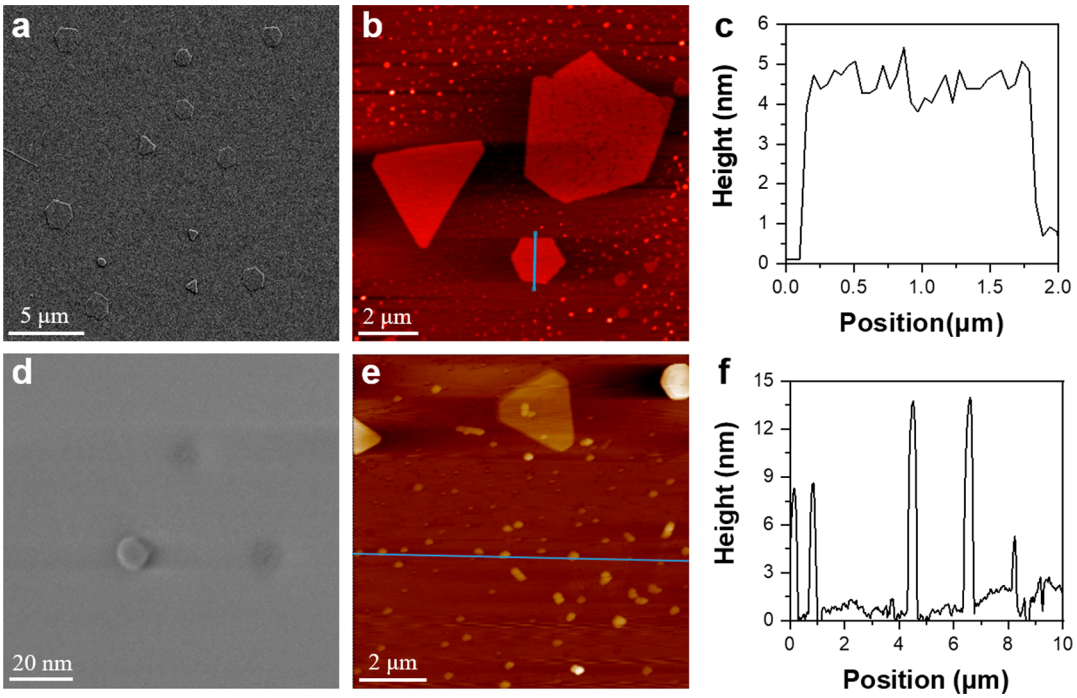

Figure 1. Structural properties of single PbI_2 flakes and nanoparticles. (a) SEM image of several single PbI_2 flakes. (b) AFM image of several single PbI_2 flakes. (c) Height profile measured across the solid line drawn in (b) for a single PbI_2 flake. (d) SEM image of a single PbI_2 nanoparticle. (e) AFM image showing the coexistence of single PbI_2 flakes and nanoparticles. (f) Height profile measured across the solid line drawn in (e) for several single PbI_2 nanoparticles.

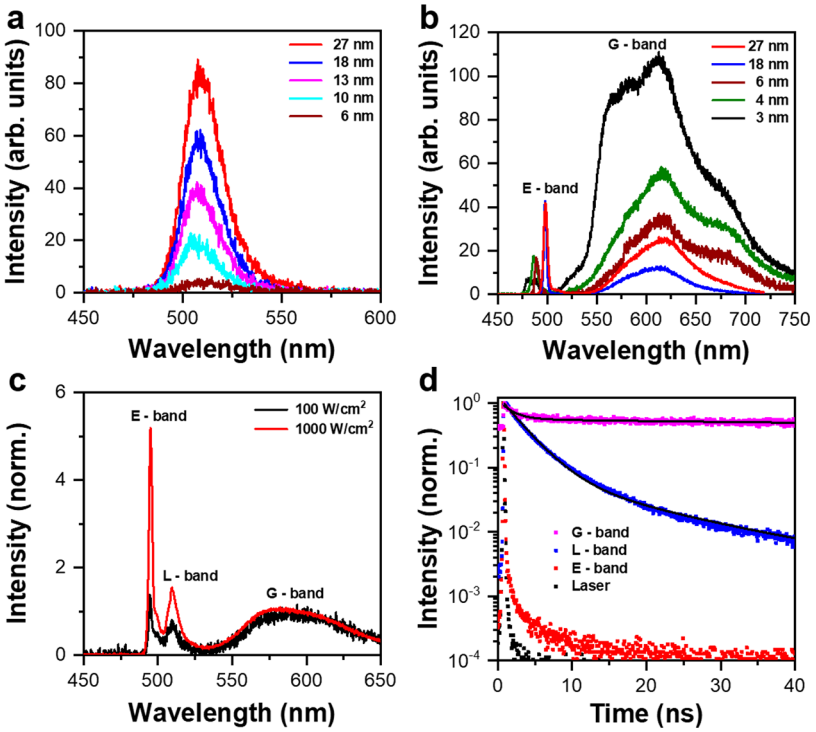

Figure 2. Optical characterizations of single PbI_2 flakes. (a) PL spectra measured at room temperature for several single PbI_2 flakes with decreasing thicknesses from ~27 to ~6 nm. (b) PL spectra measured at 4 K for several single PbI_2 flakes with decreasing thicknesses from ~27 to ~3 nm. (c) PL spectra measured at 4 K for a single PbI_2 flake excited at two laser power densities of 100 and 1000 W/cm^2, respectively. (d) PL decay curves measured at 4 K for the G-band, L-band, and E-band of the single PbI_2 flake excited at 100 W/cm^2 in (c). The PL lifetime of the E-band is very close to the system resolution estimated from the excitation laser pulse. The PL decay curves of the G-band and L-band are both fitted with biexponential functions to yield average lifetimes of ~3.96 and ~16.78 ns, respectively. The PL spectra shown in (a–c) were obtained with an integration time of 1 s.

DOI: 10.1021/acs.jpclett.9b03009
J. Phys. Chem. Lett. 2019, 10, 7863−7869

with recombination energies larger and smaller than that of the neutral single exciton, respectively.

According to an established procedure,[26] the aqueous solution of saturated PbI_2 powder was drop cast onto a plasma-treated Si/SiO_2 substrate, which was then heated to 180 °C within 5 min for the nucleation of PbI_2 flakes and nanoparticles in the ambient environment. From the scanning electron microscopy (SEM) image shown in Figure 1a, the microsized PbI_2 flakes are associated with either a hexagonal or a triangular shape, while their thicknesses range from several to hundreds of nanometers according to the atomic force microscopy (AFM) measurement. In Figure 1b, we present the AFM image of several representative PbI_2 flakes, the thickness for one of which is estimated to be ∼4 nm from its height profile plotted in Figure 1c. In addition to the above flake structures, single PbI_2 nanoparticles with a lateral size around 10 nm could also be resolved from the high-resolution SEM measurement (Figure 1d). Corresponding to the solid line drawn across the AFM image in Figure 1e, the height profile is plotted in Figure 1f for several single PbI_2 nanoparticles whose thicknesses are within the ∼5−20 nm range. The ability to grow few-layer PbI_2 flakes and nanoparticles has thus rendered us an unprecedented opportunity to explore how the fundamental optical properties of 2D semiconductors evolve with the size reduction in both the vertical and lateral dimensions.

For optical characterizations of single PbI_2 flakes at room temperature, the output beam from either a 488 nm cw laser or a 405 nm picosecond diode laser with a repetition rate of 5 MHz was focused onto the sample substrate with a power density of 100 W/cm^2, unless otherwise specified in the text. The PL signal of a single PbI_2 flake was collected by the same objective and sent through a 0.5 m spectrometer to a charge-coupled device camera for the PL spectral measurements. The PL signal of a single PbI_2 flake could be alternatively sent through a nonpolarizing 50/50 beam splitter to two avalanche photodiodes in a time-correlated single-photon counting system with a time resolution of ∼200 ps. For the low-temperature optical characterizations of single PbI_2 flakes and nanoparticles, very similar optical setups to those described above were employed except that the sample substrate was contained in a helium-free cryostat operated at 4 K.

Due to the large lateral size beyond several microns, the same single PbI_2 flake could be located from both the AFM and optical microscopy images, making it easy for us to determine the thickness-dependent PL characteristics. From the room-temperature PL spectra shown in Figure 2a for several single PbI_2 flakes, the PL peak shifts continuously from ∼509 to ∼505 nm with deceasing thickness from ∼27 to ∼6 nm. Given the bulk Bohr diameter of ∼3.8 nm,[27] the single PbI_2 flakes studied here should fall within the weak regime of vertical quantum confinement, which is slightly enhanced by the thickness reduction to cause a small blue shift in the bandgap energy.[28−31] Accompanying the blue-shifted peak, the PL intensity drops significantly with decreasing thickness and reaches almost the background level for the single PbI_2 flake with a thickness of ∼6 nm. This weakened PL in single PbI_2 flakes can be explained by the theory developed by Rashba et al.,[32] proposing that the oscillator strength of an optical transition should be proportional to the distribution range of the exciton wave function in the weak quantum confinement regime. For thicknesses smaller than 6 nm, almost no optical emission was detected from the single PbI_2 flakes, which should be caused by either the extremely small oscillator strength[32] or the formation of an indirect bandgap.[21−24]

In the next experiment, we switched to the cryogenic temperature of 4 K to perform further optical characterizations of single PbI_2 flakes, whose PL spectra are plotted in Figure 2b for several representative thicknesses and are each composed of two emission peaks denoted by E-band and G-band, respectively. Similar to the room-temperature case, the narrow E-band with a PL line width of ∼5 nm (∼25 meV) shifts slightly from ∼498.3 to ∼488.5 nm when the flake thickness is decreased from ∼27 to ∼6 nm. The PL spectra of single PbI_2 flakes with smaller thicknesses of ∼4 and ∼3 nm can also be detected, where the E-band peak is shifted further to the blue side to reach ∼485.7 and ∼481.3 nm, respectively. In contrast to the single PbI_2 flakes with larger thicknesses, the E-band PL intensity is relatively lower for the three-layer flake with a ∼3 nm thickness,[24] which should be the critical value for the direct-to-indirect bandgap transition.[21−23,25] To the lower-energy side of the E-band, there always exists a very broad G-band covering the wavelength range from ∼525 to 725 nm, and its PL intensity gets strongly enhanced with decreasing thickness of the single PbI_2 flake. In some of the studied single PbI_2 flakes, we could occasionally resolve an additional L-band with a PL peak lying between those of the E-band and G-band (Figure 2c), thus reflecting the structural inhomogeneities introduced during the flake formation process.

The E-band can be unambiguously attributed to the intrinsic exciton recombination because its PL peak energy of ∼2.5 eV is close to those values obtained previously for the bandgap energy of few-layer PbI_2 flakes.[22,23,25] According to the optical studies of ensemble PbI_2 nanoparticles embedded in porous silica films,[28,33,34] the L-band and G-band could be attributed to donor−acceptor recombination from the stoichiometric defects at the interior and surface sites, respectively. With increasing temperature, the thermal energy would be large enough to separate charge carriers from these binding defect sites, thus explaining that the L-band and G-band can only be observed at cryogenic temperatures. Because of the large surface-to-volume ratio, the G-band is dominant in the PL spectrum of a single PbI_2 flake excited at the laser power density of 100 W/cm^2 (Figure 2b). At the laser power density of 1000 W/cm^2, to completely saturate the G-band and partially saturate the L-band in Figure 2c, the E-band becomes dominant instead in the PL spectrum. The above saturation behaviors of the L-band and G-band in single PbI_2 flakes are reminiscent of those demonstrated by the defect sites in 2D TMDCs, which originate from the anion vacancies in the MoS_2, $MoSe_2$, and WSe_2 cases.[35] As shown in Figure 2d, the donor−acceptor recombination nature of the L-band and G-band is also reflected in their relatively long PL lifetimes of ∼3.96 and ∼16.78 ns, respectively, which are consistent with previous observations from the time-resolved measurements of ensemble PbI_2 nanoparticles.[33] When considering the sub-nanosecond lifetimes normally measured for the intrinsic excitons of various PbI_2 materials[30,33,36] and their fast relaxation processes into the L-band and G-band, it is reasonable to see in Figure 2d that the E-band of a single PbI_2 flake is associated with an extremely fast lifetime that is limited by our system resolution of ∼200 ps.

After studying the few-layer single PbI_2 flakes, we then moved to their nanoparticle counterparts to reveal how the lateral confinement is manifested in the optical properties measured at 4 K. For the single PbI_2 nanoparticle whose SEM

DOI: 10.1021/acs.jpclett.9b03009
J. Phys. Chem. Lett. 2019, 10, 7863−7869

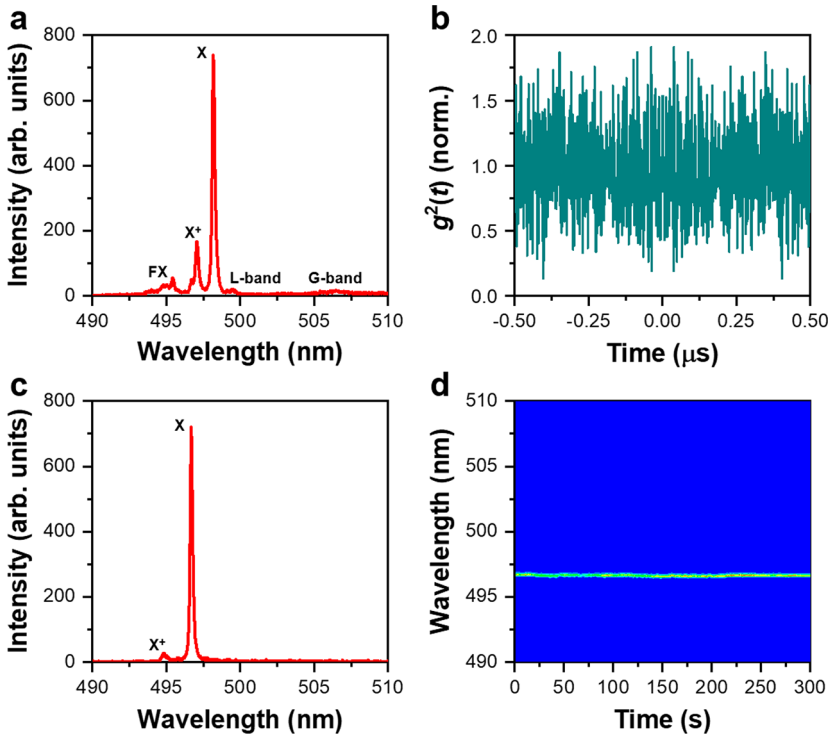

Figure 3. Optical characterizations of single PbI_2 nanoparticles at 4 K. (a) PL spectrum measured for a representative single PbI_2 nanoparticle with a complete set of FX, X^+, X, L-band, and G-band peaks. (b) Second-order photon correlation $g^2(t)$ measurement on the X peak of a single PbI_2 nanoparticle excited by a cw 488 nm laser. The missing dip at $t = 0$ confirms that it does not behave as a single-photon emitter. (c) PL spectrum measured for a single PbI_2 nanoparticle with the presence of only the X and X^+ peaks. (d) Time-dependent PL spectral image acquired for the X peak of this single PbI_2 nanoparticle with good optical stability. The PL spectra shown in (a), (c), and (d) were obtained with an integration time of 1 s.

image is shown in Figure 1d with a lateral dimension of ~10 nm, the vertical thickness was characterized to be ~20 nm from the AFM measurement. As shown in Figure 3a, the PL spectrum measured for this single PbI_2 nanoparticle contains several PL peaks denoted by FX, X^+, and X, respectively. Meanwhile, the L-band and G-band observed obviously in single PbI_2 flakes are strongly suppressed here, suggesting improved crystal quality in the single PbI_2 nanoparticles. In analogy to the assignments made previously in other PbI_2 materials,[18,28,34,37−39] the highest-energy FX peak and the dominant X peak could arise from the free excitons and the excitons bound to residual defect sites, respectively. The X peak has a center wavelength of ~498.2 nm and a PL line width of ~930 μeV, which fall within the respective ranges of ~490−500 nm and <1 meV for all of the single PbI_2 nanoparticles studied in our experiment. Compared to the E-band peaks shown in Figure 2b for single PbI_2 flakes, the bandgap energy of single PbI_2 nanoparticles shows no further blue shift, but the reinforced lateral confinement does result in a significant narrowing of the PL line width. The PL lifetimes measured for the FX, X^+, and X peaks of a single PbI_2 nanoparticle are still too fast to be resolved by our system resolution, and no single-photon emission is demonstrated from the second-order $g^2(t)$ correlation measurement of the main X peak (Figure 3b).

In the PL spectrum shown in Figure 3c for another single PbI_2 nanoparticle, the X^+ peak has a much lower PL intensity than that of the X peak with a PL line width of ~553 μeV, while all other PL peaks are completely missing. From the time-dependent PL spectral image plotted in Figure 3d, the X peak possesses superior optical stability without suffering from the PL blinking and spectral diffusion effects commonly observed in single colloidal CdSe nanocrystals.[40,41] With the increasing laser power density in Figure 4a, the X and X^+ peaks could exhibit alternative dominance in the PL spectrum at different time periods, which suggests that the X^+ peak should originate from the optical emission of a charged exciton species.[42] It is obvious that the charging probability has a positive correlation with the laser power density, as can be seen from the two representative PL spectra plotted in Figure 4b for this single PbI_2 nanoparticle excited at 100 and 5000 W/cm^2, respectively. In traditional CdSe nanocrystals, the photoexcited hole (electron) is assumed to be more localized (delocalized) due to its larger (smaller) effective mass.[43] In a photocharging event, the hole is more likely to receive the exciton recombination energy in an Auger process so that it would be pumped out of the nanocrystal, leaving behind a negatively charged core.[44] Because of the much larger electron effective mass,[28,30,36] we simply assume that the PbI_2 nanoparticles tend to be positively charged to yield the X^+ peak, which is consistent with the p-type doping configuration normally adopted by the PbI_2 materials in the synthesis process.[18] For the PL spectra shown in Figure 4b, the energy separation between the X and X^+ peaks is about −6.76 meV, while an average value of −7.44 ± 0.50 meV could be obtained from the X and X^+ peaks measured for several single PbI_2 nanoparticles. This negative binding energy for the X^+ peak strongly suggests that a repulsive interaction exists between the exciton and the extra hole,[45] which is caused by the delocalized nature of the hole according to a previous calculation.[46]

In addition to the blue-shifted X^+ peak, we could also detect a red-shifted XX peak with the high-power laser excitation, as

DOI: 10.1021/acs.jpclett.9b03009
J. Phys. Chem. Lett. 2019, 10, 7863−7869

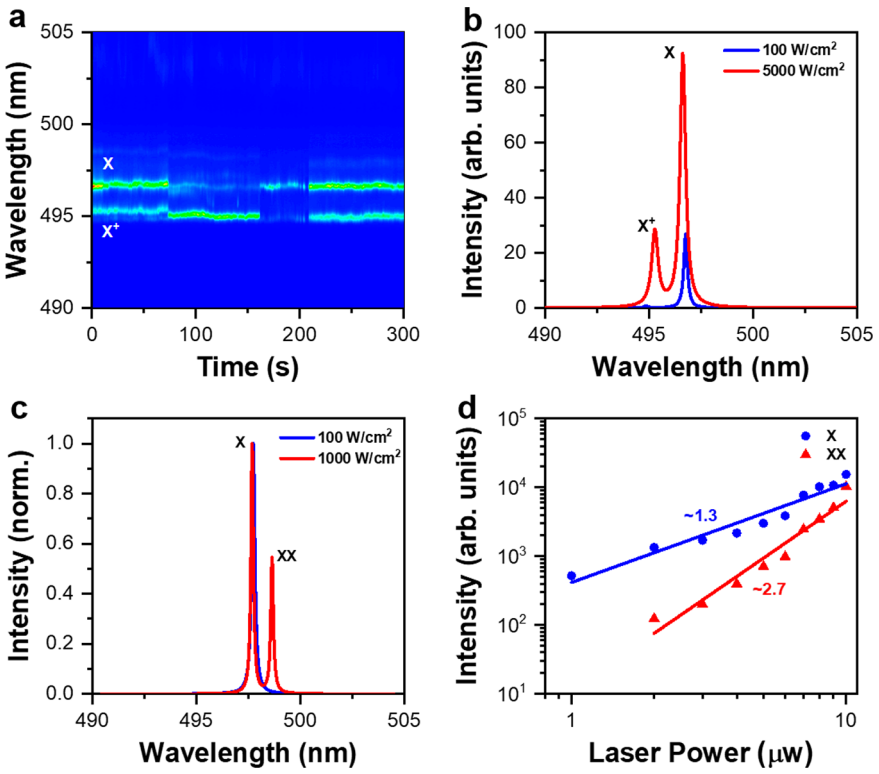

Figure 4. Charged excitons and biexcitons of single PbI_2 nanoparticles measured at 4 K. (a) Time-dependent PL spectral image of a single PbI_2 nanoparticle excited at 5000 W/cm^2, showing the existence of both X and X^+ peaks. (b) PL spectra of this single PbI_2 nanoparticle excited at two laser power densities of 100 and 5000 W/cm^2, respectively. (c) PL spectra measured for a single PbI_2 nanoparticle at two laser power densities of 100 and 1000 W/cm^2, respectively, showing the appearance of the XX peak in the latter case. (d) PL intensities of the X and XX peaks measured for this single PbI_2 nanoparticle as a function of the laser excitation power. The solid lines are power-law fittings of the X and XX data points with slope values of ∼1.3 and ∼2.7, respectively. The PL spectra shown in (a−c) were obtained with an integration time of 1 s.

can be seen in Figure 4c from the PL spectra measured for a representative single PbI_2 nanoparticle. In Figure 4d, we plot the X and XX PL intensities as a function of the laser excitation power, which can both be fitted with power-law functions to yield the slope values of ∼1.3 and ∼2.7, respectively. On the basis of its superquadratic dependence on the laser excitation power, we can attribute the XX peak to the optical emission from neutral biexcitons, just like in the cases of 2D TMDCs[10] and single CdSe nanocrystals.[47] The energy separation between the X and XX peaks is estimated to be ∼4.50 meV from the PL spectra shown in Figure 4c, while an average value of ∼7.90 ± 2.91 meV could be obtained from the X and XX peaks measured for several single PbI_2 nanoparticles. The positive binding energy of the XX peak suggests the existence of attractive interactions between the two composing excitons, which agrees well with previous biexciton studies in the PbI_2 materials.[48,49] It should be pointed out that we cannot rule out the possibility of creating even higher-order excitons whose PL peaks overlap with that of the XX, which might explain the slope of 2.7 measured in our experiment for the laser power dependence of the XX PL intensity.

To summarize, we have synthesized few-layer PbI_2 flakes and nanoparticles from the solution method and made detailed optical characterizations of these novel 2D semiconductors at the single-particle level. In contrast to the 2D TMDCs that are attractive mainly at the monolayer scale, the single PbI_2 flakes are emissive at a wide range of layer thicknesses, thus providing useful information on how the bandgap energy and associated optical properties of 2D semiconductors are influenced by the vertical quantum confinement. With the additional quantum confinement along the lateral direction, the single PbI_2 nanoparticles exhibit very succinct PL spectra with the appearances of the X (neutral single exciton), X^+ (charged single exciton), and XX (neutral biexciton) peaks. The combination of an ultranarrow PL line width of ∼1 meV with the missing single-photon emission, which is rarely observed in other semiconductor nanostructures, has rendered single PbI_2 nanoparticles a unique material platform where the vertical and lateral quantum confinements can be combined to jointly determine the exciton energy-level structures and recombination dynamics. We are optimistic that by continuously polishing the synthesis procedures of single PbI_2 nanoparticles their energy-level structures could be pushed more to the artificial-atom regime for the realization of free-standing single-photon emitters with mixed 2D and 0D quantum confinements.

AUTHOR INFORMATION

Corresponding Authors

*E-mail: wxiaoyong@nju.edu.cn (X.W.).
*E-mail: iamlwang@njtech.edu.cn (L.W.).
*E-mail: mxiao@uark.edu (M.X.).

ORCID

Yong Zhou: 0000-0002-9480-2586
Chunfeng Zhang: 0000-0001-9030-5606
Xiaoyong Wang: 0000-0003-1147-0051

Notes

The authors declare no competing financial interest.

DOI: 10.1021/acs.jpclett.9b03009
J. Phys. Chem. Lett. 2019, 10, 7863−7869

■ ACKNOWLEDGMENTS

This work is supported by the National Key R&D Program of China Grants 2019YFA0308704 and 2017YFA0303700, the National Natural Science Foundation of China Grants 61974058, 91833302, 61801210, 11574147, and 11621091, the Natural Science Foundation of Jiangsu Province Grant BK20180686, and the PAPD of Jiangsu Higher Education Institutions.

■ REFERENCES

(1) Xu, M.; Liang, T.; Shi, M.; Chen, H. Graphene-like two-dimensional materials. *Chem. Rev.* **2013**, *113*, 3766−3798.
(2) Castellanos-Gomez, A. Why all the fuss about 2D semiconductors? *Nat. Photonics* **2016**, *10*, 202−204.
(3) Novoselov, K. S.; Geim, A. K.; Morozov, S. V.; Jiang, D.; Zhang, Y.; Dubonos, S. V.; Grigorieva, I. V.; Firsov, A. A. Electric field effect in atomically thin carbon films. *Science* **2004**, *306*, 666−669.
(4) Pakdel, A.; Zhi, C.; Bando, Y.; Golberg, D. Low-dimensional boron nitride nanomaterials. *Mater. Today* **2012**, *15*, 256−265.
(5) Mak, K. F.; Lee, C.; Hone, J.; Shan, J.; Heinz, T. F. Atomically thin MoS_2: A new direct-gap semiconductor. *Phys. Rev. Lett.* **2010**, *105*, 136805.
(6) Splendiani, A.; Sun, L.; Zhang, Y.; Li, T.; Kim, J.; Chim, C.-Y.; Galli, G.; Wang, F. Emerging photoluminescence in monolayer MoS_2. *Nano Lett.* **2010**, *10*, 1271−1275.
(7) Zeng, H.; Dai, J.; Yao, W.; Xiao, D.; Cui, X. Valley polarization in MoS_2 monolayers by optical pumping. *Nat. Nanotechnol.* **2012**, *7*, 490−493.
(8) Mak, K. F.; He, K.; Lee, C.; Lee, G. H.; Hone, J.; Heinz, T. F.; Shan, J. Tightly bound trions in monolayer MoS_2. *Nat. Mater.* **2013**, *12*, 207−211.
(9) You, Y.; Zhang, X.-X.; Berkelbach, T. C.; Hybertsen, M. S.; Reichman, D. R.; Heinz, T. F. Observation of biexcitons in monolayer WSe_2. *Nat. Phys.* **2015**, *11*, 477−482.
(10) Li, Z.; Wang, T.; Lu, Z.; Jin, C.; Chen, Y.; Meng, Y.; Lian, Z.; Taniguchi, T.; Watanabe, K.; Zhang, S.; Smirnov, D.; Shi, S.-F. Revealing the biexciton and trion-exciton complexes in BN encapsulated WSe_2. *Nat. Commun.* **2018**, *9*, 3719.
(11) Li, L.; Yu, Y.; Ye, G. J.; Ge, Q.; Ou, X.; Wu, H.; Feng, D.; Chen, X. H.; Zhang, Y. Black phosphorus field-effect transistors. *Nat. Nanotechnol.* **2014**, *9*, 372−377.
(12) Dou, L.; Wong, A. B.; Yu, Y.; Lai, M.; Kornienko, N.; Eaton, S. W.; Fu, A.; Bischak, C. G.; Ma, J.; Ding, T.; Ginsberg, N. S.; Wang, L.-W.; Alivisatos, A. P.; Yang, P. Atomically thin two-dimensional organic-inorganic hybrid perovskites. *Science* **2015**, *349*, 1518−1521.
(13) Cahangirov, S.; Topsakal, M.; Aktürk, E.; Sahin, H.; Ciraci, S. Two- and one-dimensional honeycomb structures of silicon and germanium. *Phys. Rev. Lett.* **2009**, *102*, 236804.
(14) Sahin, H.; Cahangirov, S.; Topsakal, M.; Bekaroglu, E.; Aktürk, E.; Senger, R. T.; Ciraci, S. Monolayer honeycomb structures of group-IV elements and III-V binary compounds: First-principles calculations. *Phys. Rev. B: Condens. Matter Mater. Phys.* **2009**, *80*, 155453.
(15) Gähwiller, Ch.; Harbeke, G. Excitonic effects in the electroreflectance of lead iodide. *Phys. Rev.* **1969**, *185*, 1141−1149.
(16) Schlüter, I. Ch.; Schlüter, M. Electronic structure and optical properties of PbI_2. *Phys. Rev. B* **1974**, *9*, 1652−1663.
(17) Street, R. A.; Ready, S. E.; Van Schuylenbergh, K.; Ho, J.; Boyce, J. B.; Nylen, P.; Shah, K.; Melekhov, L.; Hermon, H. Comparison of PbI_2 and HgI_2 for direct detection active matrix x-ray image sensors. *J. Appl. Phys.* **2002**, *91*, 3345−3355.
(18) Zhang, J.; Song, T.; Zhang, Z.; Ding, K.; Huang, F.; Sun, B. Layered ultrathin PbI_2 single crystals for high sensitivity flexible photodetectors. *J. Mater. Chem. C* **2015**, *3*, 4402−4406.
(19) Zheng, W.; Zhang, Z.; Lin, R.; Xu, K.; He, J.; Huang, F. High-crystalline 2D layered PbI_2 with ultrasmooth surface: Liquid-phase synthesis and application of high-speed photon detection. *Adv. Electron. Mater.* **2016**, *2*, 1600291.
(20) Lee, M. M.; Teuscher, J.; Miyasaka, T.; Murakami, T. N.; Snaith, H. J. Efficient hybrid solar cells based on meso-superstructured organometal halide perovskites. *Science* **2012**, *338*, 643−647.
(21) Zhou, M.; Duan, W.; Chen, Y.; Du, A. Single layer lead iodide: Computational exploration of structural, electronic and optical properties, strain induced band modulation and the role of spin-orbital-coupling. *Nanoscale* **2015**, *7*, 15168−15173.
(22) Toulouse, A. S.; Isaacoff, B. P.; Shi, G.; Matuchová, M.; Kioupakis, E.; Merlin, R. Frenkel-like Wannier-Mott excitons in few-layer PbI_2. *Phys. Rev. B: Condens. Matter Mater. Phys.* **2015**, *91*, 165308.
(23) Frisenda, R.; Island, J. O.; Lado, J. L.; Giovanelli, E.; Gant, P.; Nagler, P.; Bange, S.; Lupton, J. M.; Schüller, C.; Molina-Mendoza, A. J.; Aballe, L.; Foerster, M.; Korn, T.; Angel Niño, M.; Perez de Lara, D.; Pérez, E. M.; Fernandéz-Rossier, J.; Castellanos-Gomez, A. Characterization of highly crystalline lead iodide nanosheets prepared by room-temperature solution processing. *Nanotechnology* **2017**, *28*, 455703.
(24) Yagmurcukardes, M.; Peeters, F. M.; Sahin, H. Electronic and vibrational properties of PbI_2: From bulk to monolayer. *Phys. Rev. B: Condens. Matter Mater. Phys.* **2018**, *98*, 085431.
(25) Zhong, M.; Zhang, S.; Huang, L.; You, J.; Wei, Z.; Liu, X.; Li, J. Large-scale 2D PbI_2 monolayers: Experimental realization and their indirect band-gap related properties. *Nanoscale* **2017**, *9*, 3736−3741.
(26) Sun, Y.; Zhou, Z.; Huang, Z.; Wu, J.; Zhou, L.; Cheng, Y.; Liu, J.; Zhu, C.; Yu, M.; Yu, P.; Zhu, W.; Liu, Y.; Zhou, J.; Liu, B.; Xie, H.; Cao, Y.; Li, H.; Wang, X.; Liu, K.; Wang, X.; Wang, J.; Wang, L.; Huang, W. Band structure engineering of interfacial semiconductors based on atomically thin lead iodide crystals. *Adv. Mater.* **2019**, *31*, 1806562.
(27) Nagamune, Y.; Takeyama, S.; Miura, N. Magnetoabsorption spectra of band-edge excitons in 2*H*-PbI_2 at high magnetic fields up to 40 T. *Phys. Rev. B: Condens. Matter Mater. Phys.* **1989**, *40*, 8099−8102.
(28) Lifshitz, E.; Yassen, M.; Bykov, L.; Dag, I.; Chaim, R. Nanometer-sized particles of PbI_2 embedded in SiO_2 films. *J. Phys. Chem.* **1994**, *98*, 1459−1463.
(29) Saito, S.; Goto, T. Spatial-confinement effect on phonons and excitons in PbI_2 microcrystallites. *Phys. Rev. B: Condens. Matter Mater. Phys.* **1995**, *52*, 5929−5934.
(30) Yamamoto, A.; Nakahara, H.; Yoshihara, M.; Goto, T. Transformation from a weak to strong-size confinement regime in PbI_2 ultra-thin microcrystallites embedded in E-MAA copolymer. *J. Phys. Soc. Jpn.* **1998**, *67*, 2120−2124.
(31) Goto, T.; Saito, S.; Tanaka, M. Size quantization of excitons in PbI_2 microcrystallites. *Solid State Commun.* **1991**, *80*, 331−334.
(32) Rashba, E. I.; Gurgenishvili, G. E. Edge absorption theory in semiconductors. *Sov. Phys. Solid State* **1962**, *4*, 759−760.
(33) Dag, I.; Lifshitz, E. Dynamics of recombination processes in PbI_2 nanocrystals embedded in porous silica films. *J. Phys. Chem.* **1996**, *100*, 8962−8972.
(34) Lifshitz, E.; Bykov, L.; Yassen, M.; Chen-Esterlit, Z. The investigation of donor and acceptor states in nanoparticles of the layered semiconductor PbI_2. *Chem. Phys. Lett.* **1997**, *273*, 381−388.
(35) Tongay, S.; Suh, J.; Ataca, C.; Fan, W.; Luce, A.; Kang, J. S.; Liu, J.; Ko, C.; Raghunathanan, R.; Zhou, J.; Ogletree, F.; Li, J.; Grossman, J. C.; Wu, J. Defects activated photoluminescence in two-dimensional semiconductors: Interplay between bound, charged, and free excitons. *Sci. Rep.* **2013**, *3*, 2657.
(36) Sengupta, A.; Jiang, B.; Mandal, K. C.; Zhang, J. Z. Ultrafast electronic relaxation dynamics in PbI_2 semiconductor colloidal nanoparticles: A femtosecond transient absorption study. *J. Phys. Chem. B* **1999**, *103*, 3128−3137.
(37) Cong, C.; Shang, J.; Niu, L.; Wu, L.; Chen, Y.; Zou, C.; Feng, S.; Qiu, Z.-J.; Hu, L.; Tian, P.; Liu, Z.; Yu, T.; Liu, R. Anti-stokes photoluminescence of van der waals layered semiconductor PbI_2. *Adv. Opt. Mater.* **2017**, *5*, 1700609.
(38) Condeles, J. F.; Ando, R. A.; Mulato, M. Optical and structural properties of PbI_2 thin films. *J. Mater. Sci.* **2008**, *43*, 525−529.

DOI: 10.1021/acs.jpclett.9b03009
J. Phys. Chem. Lett. 2019, 10, 7863−7869

(39) Skolnick, M. S.; Bimberg, D. Angular-dependent magneto-luminescence study of the layer compound 2*H*-PbI_2. *Phys. Rev. B: Condens. Matter Mater. Phys.* **1978**, *18*, 7080−7088.
(40) Nirmal, M.; Dabbousi, B. O.; Bawendi, M. G.; Macklin, J. J.; Trautman, J. K.; Harris, T. D.; Brus, L. E. Fluorescence intermittency in single cadmium selenide nanocrystals. *Nature* **1996**, *383*, 802−804.
(41) Empedocles, S. A.; Norris, D. J.; Bawendi, M. G. Photo-luminescence spectroscopy of single CdSe nanocrystallite quantum dots. *Phys. Rev. Lett.* **1996**, *77*, 3873−3876.
(42) Yin, C.; Chen, L.; Song, N.; Lv, Y.; Hu, F.; Sun, C.; Yu, W. W.; Zhang, C.; Wang, X.; Zhang, Y.; Xiao, M. Bright-exciton fine structure splittings in single perovskite nanocrystals. *Phys. Rev. Lett.* **2017**, *119*, 026401.
(43) Gómez, D. E.; van Embden, J.; Mulvaney, P.; Fernée, M. J.; Rubinsztein-Dunlop, H. Exciton-trion transitions in single CdSe-CdS core-shell nanocrystals. *ACS Nano* **2009**, *3*, 2281−2287.
(44) Hu, F.; Zhang, Q.; Zhang, C.; Wang, X.; Xiao, M. Charged two-exciton emission from a single semiconductor nanocrystal. *Appl. Phys. Lett.* **2015**, *106*, 133106.
(45) Rodt, S.; Schliwa, A.; Pötschke, K.; Guffarth, F.; Bimberg, D. Correlation of structural and few-particle properties of self-organized InAs/GaAs quantum dots. *Phys. Rev. B: Condens. Matter Mater. Phys.* **2005**, *71*, 155325.
(46) Findeis, F.; Baier, M.; Zrenner, A.; Bichler, M.; Abstreiter, G.; Hohenester, U.; Molinari, E. Optical excitations of a self-assembled artificial ion. *Phys. Rev. B: Condens. Matter Mater. Phys.* **2001**, *63*, 121309.
(47) Louyer, L.; Biadala, L.; Trebbia, J.-B.; Fernée, M. J.; Tamarat, Ph.; Lounis, B. Efficient biexciton emission in elongated CdSe/ZnS nanocrystals. *Nano Lett.* **2011**, *11*, 4370−4375.
(48) Makino, T.; Gu, P.; Watanabe, M.; Hayashi, T. Excitation-energy dependence of biexciton formation efficiency in PbI_2. *Solid State Commun.* **1995**, *93*, 983−987.
(49) Ando, M.; Yazaki, M.; Katayama, I.; Ichida, H.; Wakaiki, S.; Kanematsu, Y.; Takeda, J. Photoluminescence dynamics due to biexcitons and exciton-exciton scattering in the layered-type semi-conductor PbI_2. *Phys. Rev. B: Condens. Matter Mater. Phys.* **2012**, *86*, 155206.

DOI: 10.1021/acs.jpclett.9b03009
J. Phys. Chem. Lett. 2019, 10, 7863−7869